

# Measurement-based Analysis of Relaying Performance for Vehicle-to-Vehicle Communications with Large Vehicle Obstructions

Ruisi He<sup>1,2</sup>, Andreas F. Molisch<sup>2</sup>, Fredrik Tufvesson<sup>3</sup>, Rui Wang<sup>2</sup>, Tingting Zhang<sup>4</sup>,  
Zheda Li<sup>2</sup>, Zhangdui Zhong<sup>1</sup>, and Bo Ai<sup>1</sup>

<sup>1</sup>State Key Laboratory of Rail Traffic Control and Safety, Beijing Jiaotong University, Beijing, China

<sup>2</sup>Department of Electrical Engineering, University of Southern California, Los Angeles, USA

<sup>3</sup>Department of Electrical and Information Technology, Lund University, Lund, Sweden

<sup>4</sup>Harbin Institute of Technology, Shenzhen Graduate School, Shenzhen, China

Email: ruisi.he@ieee.org

**Abstract**—It has been widely recognized that relaying is an important method for increasing the reliability and spectral efficiency of communications systems, and it is thus helpful for improving the performance of vehicle-to-vehicle (V2V) communication systems. However, designing and evaluating V2V relay networks require understanding the effect of shadowing, as this critically impacts the performance of the relay system. Even though the theoretic performances of various relaying schemes have been well investigated, there is a lack of empirical test that incorporates realistic shadowing effects. In this paper, we analyze the performance of relaying transmission in V2V scenarios based on measurements in scenarios where shadowing occurs through large vehicles such as buses. We investigate several potential locations for the relay nodes, and the measurements are performed with two static transmitters (TX) and one dynamic receiver (RX). Outage probabilities of several relaying schemes such as multi-hop decode-and-forward, multi-hop amplify-and-forward, and diversity-amplify-and-forward are estimated and discussed based on the measured instantaneous end-to-end signal-to-noise ratio (SNR). It is found that: (i) shadowing effect caused by the bus between V2V line-of-sight (LOS) links increases the outage probability for the non-LOS (NLOS) direct transmission; (ii) using relay node on the bus roof can significantly improve transmission, however, a strong shadowing effect may reduce the acceptable communication distance of relaying scheme; and (iii) the diversity-amplify-and-forward relaying scheme generally has the best performance. Our results can be used to design a relay system for V2V communications.

## I. INTRODUCTION

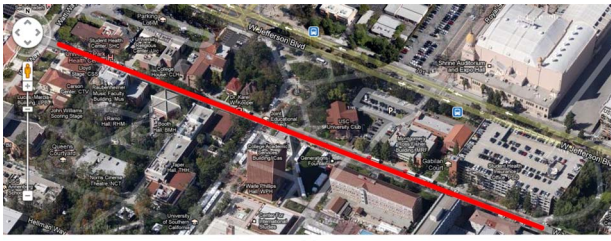
Recently, research into vehicular communications has gained strong momentum due to its wide application in the field of Intelligent Transportation Systems (ITS) [1], [2]. Reliable vehicular communication links are required to meet the strict packet delay deadlines in ITSs. Therefore, considerable efforts are devoted to improve the vehicle-to-vehicle (V2V) communication links.

Due to the movements of the vehicles, low heights of antennas, and the dynamic environments, the V2V line-of-sight (LOS) links are often blocked by other vehicles (especially some large vehicles like buses and trucks). Such a non-LOS

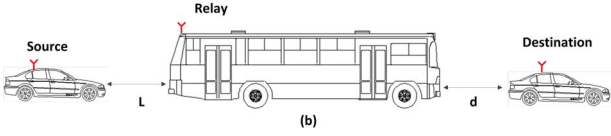
(NLOS) scenario increases the packet loss probability and thus limits the reliability of the systems. Introduction of relay nodes, which could be placed on top of large vehicles, can help to ensure dependable connectivity in those scenarios, and also improve capacity.

Many relaying techniques have been proposed, such as decode-and-forward and amplify-and-forward [3], and used for V2V communications. In [4], multi-hop decode-and-forward scheme is used to improve vehicle-to-infrastructure communications. In [5], a novel probabilistic bundle relaying scheme is proposed for vehicular network and end-to-end delay is analyzed. In [6], performance of amplify-and-forward scheme for V2V communication is investigated under cascaded Rayleigh channel. In [7], performance of decode-and-forward scheme for V2V communication is investigated under Rayleigh channel. In [8], outage performance of amplify-and-forward for inter-vehicular communication is investigated under double-Rayleigh channel. In [9], selection cooperation in decode-and-forward vehicular networks with cascaded Rayleigh fading is investigated. In [10], link level simulation for decode-and-forward relaying at road intersection is performed using a vehicular non-stationary geometry based stochastic channel model. Related work mentioned above shows that the performance of relaying schemes has been mostly analyzed by simulations under some theoretic distributions. Measurement-based investigations of realistic relay system in V2V communications, which reflect practical channel conditions, have been largely neglected in the literature.

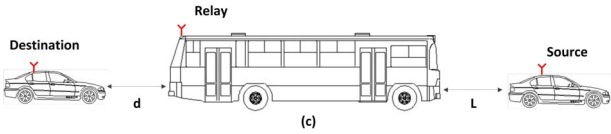
Moreover, a major factor influencing the performance enhancement by above relaying schemes is shadow fading [11], [12], which is found to significantly affect end-to-end signal-to-noise (SNR) in the scenario with large vehicular obstructions [13]. To overcome the strong shadowing effect caused by buses and trucks, suitable relaying scheme and arrangement plan of relay node are required. Thus, knowledge of the performance of various relaying schemes, suitable place to arrange relay nodes, and measurement-based analysis are



(a)



(b)



(c)



(d)

Fig. 1. Measurement scenarios. (a) Top view of the street (red line) on campus of USC. (b) Scenario 1. (c) Scenario 2. (d) Scenario 3.

essential for the development of such systems.

In conclusion, to the authors' best knowledge, there exists no experimental investigation of relaying performance in V2V scenarios with large vehicular obstructions. To fill this gap, we conduct realistic measurements in scenarios with large vehicles obstructing the LOS. We perform the measurements using a software-radio based measurement system. Outage probabilities of various relaying schemes such as multi-hop decode-and-forward, multi-hop amplify-and-forward, and diversity-amplify-and-forward are discussed based on the measured instantaneous end-to-end SNR.

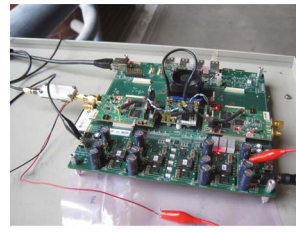
The remainder of the paper is organized as follows: Section II introduces the measurement campaign. Section III describes the system models of different relaying schemes. Section IV presents the results of outage probability, and Section V concludes the paper.

## II. MEASUREMENTS

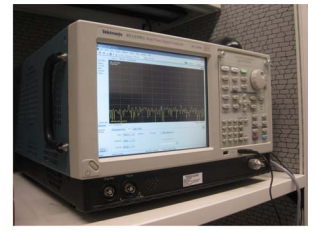
To analyze the performances of various relaying schemes, channel impulse responses are measured at different distances and instantaneous equivalent end-to-end SNRs (as reported later) are further extracted for the comparison of relaying performances. In this section, we summarize the measurement campaign and the different arrangements of relay nodes.

### A. Measurement Scenario

Measurements were conducted on the street of University of Southern California (USC), USA, as shown in Fig. 1(a). Three scenarios are considered:



(a)



(b)



(c)



(d)

Fig. 2. Measurement system. (a) WARP FPGA board. (b) Tektronix RSA5106A real-time spectrum analyzer. (c) Self-designed trigger wheel. (d) Reference measurements in an anechoic chamber.

- Scenario 1: In this scenarios, a standard America school bus is placed in the middle of two compact cars and blocks the V2V LOS communication link. The bus is 10 m long and 3 m high; both compact cars are 4.4 m long and 1.5 m high. The relay node is placed at the end of the bus roof, as shown in Fig. 1(b). The source node is placed on the roof of the compact car, which has a distance of  $L$  to the back of the bus; whereas the destination node is placed on the roof of another compact car, which has a distance of  $d$  to the front of the bus.
- Scenario 2: This scenario is similar to scenario 1. The only difference is that the source node is placed in front of bus and the destination node is at the back of bus, as shown in Fig. 1(c).
- Scenario 3: In this scenario, we conducted V2V LOS measurements without placing relay nodes, which can be used for comparison between LOS direct transmission and NLOS relaying transmission.

In the measurements, the car with source node is static and the car with destination node is dynamic, i.e.,  $L$  is fixed. Both cases of  $L = 0.1$  m and  $L = 50$  m were considered in the measurements to have more realizations for the analysis.

### B. Measurement System

Measurements were conducted at 5.8 GHz, with two WARP FPGA software radio units [14] as transmitters (TXs) and a Tektronix RSA5106A spectrum analyzer as receiver (Rx), as shown in Fig. 2. Two Zadoff-Chu sequences [3] with a 20 MHz frequency interval and a 15 MHz bandwidth are used as the transmit signals for source and relay nodes. The transmit output power is 28 dBm for both nodes. The destination node acquires the signals from source and relay at the same time. The two signals are distinguished from each other by using a filter at the baseband. We verified with a spectrum analyzer that the two signals are not interfering with each other. The

source and relay nodes are set to transmit continuously and synchronously. The destination node is connected to a trigger wheel (which has a distance resolution of 0.1 cm), as shown in Fig. 2(c), and saves the snapshots of the two transfer functions every 0.5 wavelength ( $\approx 2.5$  cm).

To remove the impact of the equipment on the measured channels, e.g., antennas, WARP boards, spectrum analyzer, reference measurements (with the same gain setting as in the measurements) at 1 m TX-RX separation distance have been conducted in an anechoic chamber, as shown in Fig. 2(d), and the measured transfer functions were calibrated by the reference measurements. A detailed description of the measurement system and data calibration can be found in [13], [15]. The instantaneous SNR can be calculated as the ratio of signal power to the noise power, which can be estimated by integrating over frequency response.

### III. SYSTEM MODEL

In this section, we present the equivalent end-to-end SNR  $\gamma_{\text{equ}}$  for various relaying schemes [3], [16]–[18], which is the basic for the later performance analysis of outage probability.

#### A. Direct Transmission

If there is no relay, the equivalent end-to-end SNR of the direct transmission can be easily expressed as

$$\gamma_{\text{equ}} = \gamma_{\text{sd}}, \quad (1)$$

where  $\gamma_{\text{sd}}$  is the SNR of source-destination link.

#### B. Multi-Hop Decode-and-Forward

For the multi-hop decode-and-forward relaying scheme, the relay receives a packet and decodes it, thus eliminating the effects of noise, before re-encoding and retransmitting the packet. Since the source-relay and relay-destination links are independent, transmission is successful only if the two independent paths (source-relay and relay-destination) both provide sufficient quality. Therefore, the equivalent end-to-end SNR of the multi-hop decode-and-forward transmission can be expressed as

$$\gamma_{\text{equ}} = \min[\gamma_{\text{sr}}, \gamma_{\text{rd}}], \quad (2)$$

where  $\gamma_{\text{sr}}$  and  $\gamma_{\text{rd}}$  is the SNRs of source-relay and relay-destination links, respectively.  $\min[\cdot]$  denotes the minimum value of  $(\cdot)$ .

#### C. Multi-hop Amplify-and-Forward

The basic principle of the multi-hop amplify-and-forward is that the relay takes the (noisy) signal that it receives and amplifies it with a gain, without decoding and demodulating. In such case, both signal and noise (of the source-relay link) are amplified and transmitter to the destination. The maximum amplification factor  $\beta$  is limited by power constraints, expressed as

$$|\beta|^2 = \frac{P_r}{P_n + P_s \cdot |h_{\text{sr}}|^2}, \quad (3)$$

where  $P_s$ ,  $P_r$ , and  $P_n$  are the powers of source, relay, and noise, respectively.  $h_{\text{sr}}$  is the channel coefficient between

source and relay.  $|\cdot|$  denotes the absolute. If we assume  $P_s = P_r = P$ , which is same to our measurement setup, the equivalent end-to-end SNR of the multi-hop amplify-and-forward transmission can be expressed as

$$\begin{aligned} \gamma_{\text{equ}} &= \frac{P|\beta h_{\text{sr}} h_{\text{rd}}|^2}{\left(|\beta h_{\text{rd}}|^2 + 1\right) \cdot P_n} \\ &= \frac{\left(\left(\frac{P}{P_n}\right) \cdot |h_{\text{sr}}|^2\right) \cdot \left(\left(\frac{P}{P_n}\right) \cdot |h_{\text{rd}}|^2\right) \cdot (P_n)^2}{P \cdot P_n \cdot \left(|h_{\text{sr}}|^2 + |h_{\text{rd}}|^2\right) + (P_n)^2} \\ &= \frac{\left(\left(\frac{P}{P_n}\right) \cdot |h_{\text{sr}}|^2\right) \cdot \left(\left(\frac{P}{P_n}\right) \cdot |h_{\text{rd}}|^2\right)}{\left(\frac{P}{P_n}\right) \cdot |h_{\text{sr}}|^2 + \left(\frac{P}{P_n}\right) \cdot |h_{\text{rd}}|^2 + 1} \\ &= \frac{\gamma_{\text{sr}} \cdot \gamma_{\text{rd}}}{\gamma_{\text{sr}} + \gamma_{\text{rd}} + 1} \end{aligned} \quad (4)$$

where  $h_{\text{rd}}$  is the channel coefficient between relay and destination.

#### D. Diversity-Amplify-and-Forward

For the diversity-amplify-and-forward relaying scheme, the signals from source and relay are combined at destination. To maximize SNR, the maximum-ratio combining is performed, and the equivalent end-to-end SNR can be expressed as

$$\begin{aligned} \gamma_{\text{equ}} &= \left(\frac{P}{P_n}\right) |h_{\text{sd}}|^2 + \frac{\left(\left(\frac{P}{P_n}\right) |h_{\text{sr}}|^2\right) \left(\left(\frac{P}{P_n}\right) |h_{\text{rd}}|^2\right)}{\left(\frac{P}{P_n}\right) |h_{\text{sr}}|^2 + \left(\frac{P}{P_n}\right) |h_{\text{rd}}|^2 + 1} \\ &= \gamma_{\text{sd}} + \frac{\gamma_{\text{sr}} \cdot \gamma_{\text{rd}}}{\gamma_{\text{sr}} + \gamma_{\text{rd}} + 1} \end{aligned} \quad (5)$$

where  $\gamma_{\text{sd}}$  and  $h_{\text{sd}}$  are the SNR and channel coefficient of the source-destination link.

## IV. ANALYSIS

In this section, we analyze outage probability using the measured instantaneous equivalent end-to-end SNR  $\gamma_{\text{equ}}$ , and discuss the performance of difference relaying schemes.

#### A. Outage Probability

In this paper, outage probability  $P_{\text{out}}$  is defined in terms of probabilities that  $\gamma_{\text{equ}}$  is below the cut-off value  $c_\gamma$  for successful reception. We first define a sliding/non-overlapped 50 wavelengths window (including 100 samples), then we calculate the cumulative distribution function (CDF)  $F$  of all the measured *instantaneous* equivalent end-to-end SNR within each window. By searching the curve of  $F$  for the SNR cut-off value  $c_\gamma$ , we can get the corresponding probability in each window, which is  $P_{\text{out}}$ , expressed as

$$P_{\text{out}} = \Pr\{\gamma_{\text{equ}} \leq c_\gamma\} = F(\gamma_{\text{equ}} = c_\gamma), \quad (6)$$

where  $\Pr\{\cdot\}$  denotes probability. In this paper,  $c_\gamma$  is set as 15 dB, according to the evaluations of frame-error-ratio for 802.11p physical layer [19]. To discuss the acceptable communication distance, the  $P_{\text{out}}$  threshold is set as 0.1 in the following; though different thresholds can be used if needed.

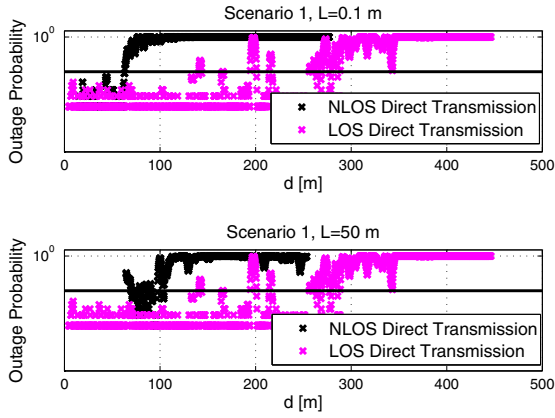


Fig. 3. NLOS direct transmission (scenario 1) vs LOS direct transmission (scenario 3). The black line represents  $P_{\text{out}} = 0.1$ .

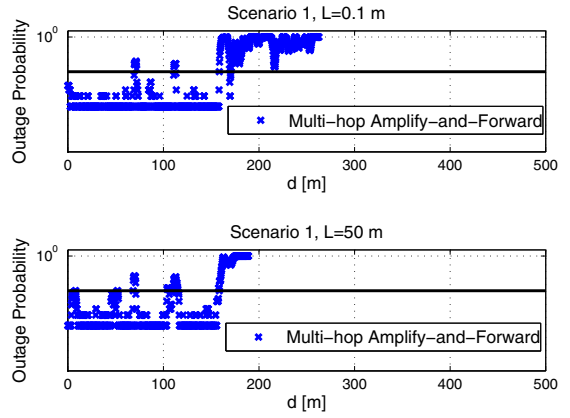


Fig. 5. Multi-hop amplify-and-forward in scenario 1. The black line represents  $P_{\text{out}} = 0.1$ .

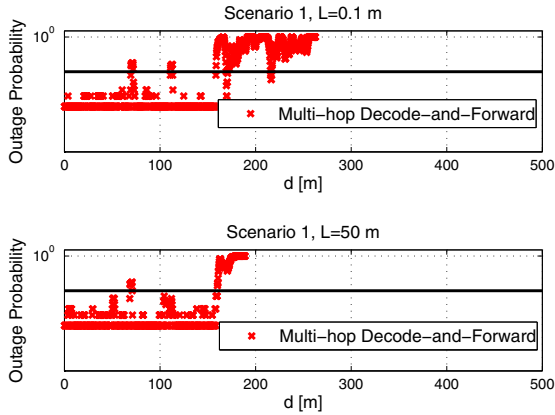


Fig. 4. Multi-hop decode-and-forward in scenario 1. The black line represents  $P_{\text{out}} = 0.1$ .

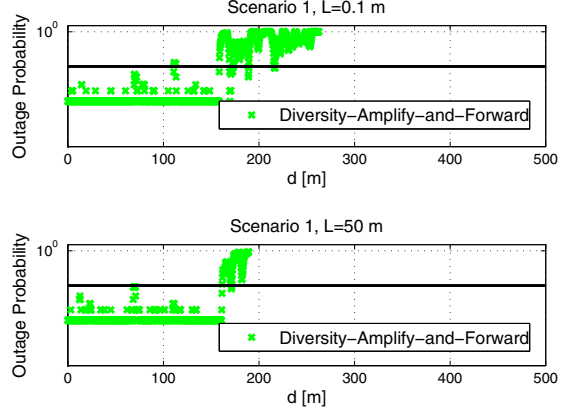


Fig. 6. Diversity-amplify-and-forward in scenario 1. The black line represents  $P_{\text{out}} = 0.1$ .

### B. Results in Scenario 1

Figs. 3-6 show the measured  $P_{\text{out}}$  vs  $d$  for different relaying schemes in scenario 1, where “NLOS Direct Transmission” and “LOS Direct Transmission” represent the links between source and destination in scenarios 1 and 3, respectively. Several observations are worth noting:

- Fig. 3 shows that the acceptable communication distance (i.e.,  $P_{\text{out}} < 0.1$ ) is 200 m and 60 m for LOS and NLOS direct transmissions, respectively. A larger distance  $L$  generally reduces the outage probability for the NLOS direct transmission, due to less shadowing [13].
- The acceptable communication distance for all the three relaying schemes is generally around 160 m.
- In Fig. 4, no clear relation between outage probability and  $L$  is observed. This is because  $\gamma_{\text{equ}}$  is mainly determined by  $\gamma_{\text{rd}}$  in such case, and  $\gamma_{\text{rd}}$  is independent of  $L$ .
- In Fig. 5, a larger  $L$  slightly increases outage probability (e.g., when  $d = 2, 50, 110$  m). This is because a larger  $L$  corresponds to a smaller  $\gamma_{\text{sr}}$ .
- In Fig. 6, no clear relation between outage probability and  $L$  is observed. This is because on one hand, a larger

$L$  increases  $\gamma_{\text{sd}}$ ; on the other hand, a larger  $L$  reduces  $\gamma_{\text{sr}}$ . Therefore, the two effects may counteract.

### C. Results in Scenario 2

Figs. 7-10 show the measured  $P_{\text{out}}$  vs  $d$  for different relaying schemes in scenario 2, where “NLOS Direct Transmission” and “LOS Direct Transmission” represent the links between source and destination in scenarios 2 and 3, respectively. Several observations are worth noting:

- Fig. 7 shows that the acceptable communication distance is 200 m for LOS direct transmission; whereas it is around 40 m and 60 m for NLOS direct transmission when  $L = 0.1$  m and  $L = 50$  m, respectively. A larger  $L$  also reduces the outage probability for the NLOS direct transmission due to less shadowing, which is the same to Fig. 3.
- The acceptable communication distance for all the three relaying schemes is around 40 m and 150 m when  $L = 0.1$  m and  $L = 50$  m, respectively.
- In Fig. 8 and Fig. 9, a larger  $L$  increases the acceptable communication distance. This is because in scenario 2, a larger  $L$  leads to a larger  $\gamma_{\text{sr}}$ .

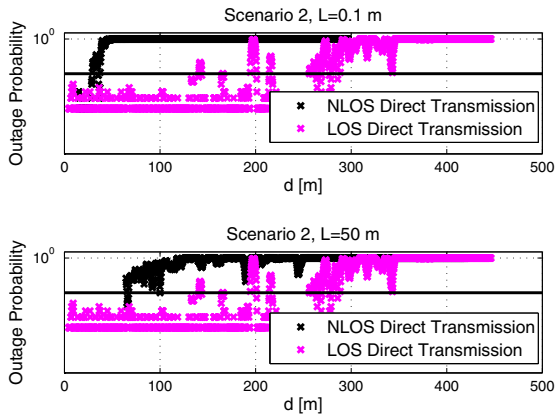


Fig. 7. NLOS direct transmission (scenario 2) vs LOS direct transmission (scenario 3). The black line represents  $P_{\text{out}} = 0.1$ .

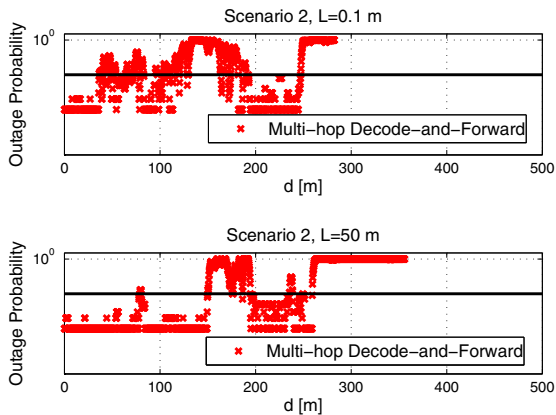


Fig. 8. Multi-hop decode-and-forward in scenario 2. The black line represents  $P_{\text{out}} = 0.1$ .

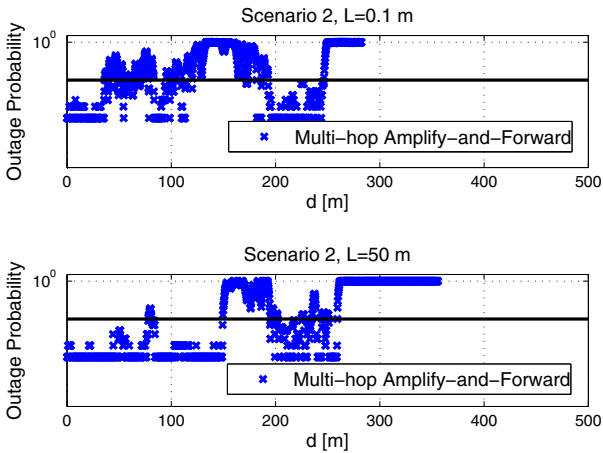


Fig. 9. Multi-hop amplify-and-forward in scenario 2. The black line represents  $P_{\text{out}} = 0.1$ .

- In Fig. 10, a larger  $L$  also increases the acceptable communication distance. This is because in scenario 2, a larger  $L$  leads to a larger  $\gamma_{\text{sd}}$  and  $\gamma_{\text{sr}}$ .

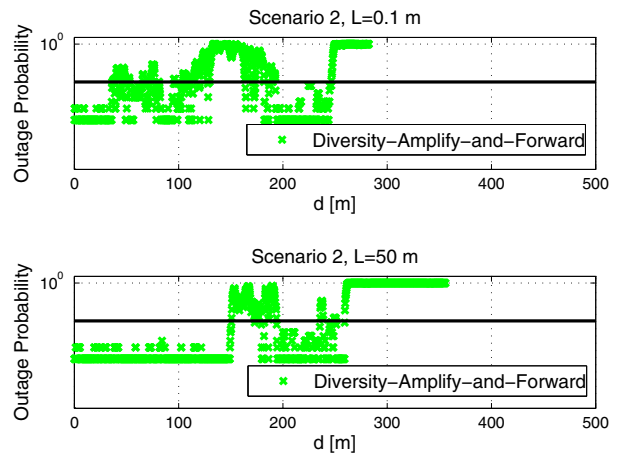


Fig. 10. Diversity-amplify-and-forward in scenario 2. The black line represents  $P_{\text{out}} = 0.1$ .

#### D. Comparison

To compare performances of the three relaying schemes, we define two difference factors  $y_1$  and  $y_2$  as follows:

$$\begin{aligned} y_1 &= P_{\text{out},\text{M-AF}} - P_{\text{out},\text{M-DF}} \\ y_2 &= P_{\text{out},\text{M-DF}} - P_{\text{out},\text{D-AF}} \end{aligned} \quad (7)$$

where  $P_{\text{out},\text{M-DF}}$ ,  $P_{\text{out},\text{M-AF}}$ , and  $P_{\text{out},\text{D-AF}}$  are outage probabilities of the multi-hop decode-and-forward, multi-hop amplify-and-forward, and diversity-amplify-and-forward schemes, respectively. Figs. 11 and 12 show comparisons of  $y_1$  and  $y_2$  in scenarios 1 and 2, respectively. It is found that both  $y_1$  and  $y_2$  are generally larger than 0, i.e.,  $P_{\text{out},\text{D-AF}} \leq P_{\text{out},\text{M-DF}} \leq P_{\text{out},\text{M-AF}}$ . We can thus conclude that the diversity-amplify-and-forward relaying scheme generally has the best performance.

We can also compare the results between scenario 1 and scenario 2, from Fig. 3 to Fig. 10. It is found that when  $L = 0.1$  m, the acceptable communication distance of the three relays in scenario 1 is generally 100 m larger than in scenario 2. This is because in scenario 2, a small  $L$  leads to a small  $\gamma_{\text{sr}}$ . When  $L = 50$  m, no significant difference between scenarios 1 and 2 for the three relays is observed<sup>1</sup>.

#### V. CONCLUSION

In this paper, we analyze the performances of various relaying schemes for V2V scenario with large bus obstruction. Some potential locations for relay nodes to improve the communication are tested. Outage probabilities of LOS and NLOS direct transmissions, multi-hop decode-and-forward, multi-hop amplify-and-forward, and diversity-amplify-and-forward are estimated based on the realistic measurements. It is found that:

- The acceptable communication distance for NLOS direct transmission (i.e., with bus obstruction) is generally 150 m less than LOS direct transmission. A less pronounced

<sup>1</sup>Note that in the measurements, the range of  $d$  is different for scenario 1 and scenario 2, due to implementation issue.

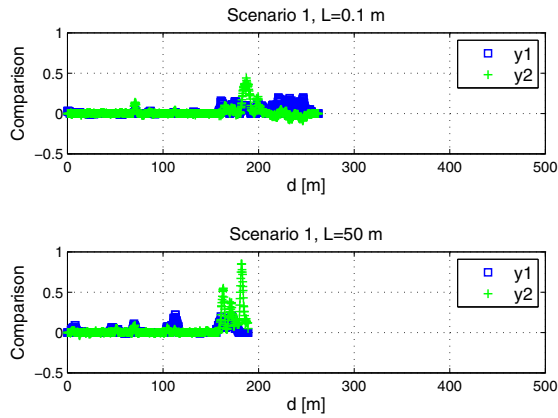


Fig. 11. Comparison of  $y_1$  and  $y_2$  in scenario 1.

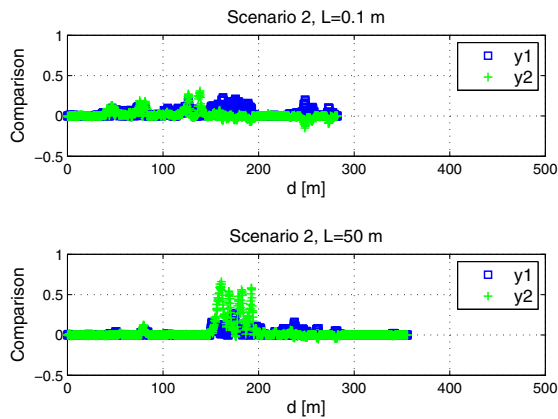


Fig. 12. Comparison of  $y_1$  and  $y_2$  in scenario 2.

shadowing effect (i.e., large  $L$ ) generally reduces the outage probability for the NLOS direct transmission.

- By placing relay node on the bus roof, the acceptable communication distance for NLOS relaying transmission is only 40 m less than the LOS direct transmission. However, a strong shadowing effect may lead to small  $\gamma_{sr}$  (e.g., scenario 2 when  $L = 0.1$  m) and thus reduces the acceptable communication distance.
- Comparison between two scenarios shows that the scenario 1 generally has better performance, i.e., the relay node should be placed close to source.
- Comparison among three relaying schemes shows that the diversity-amplify-and-forward relaying scheme generally has the best performance.

The results in this paper show the empirical impact of shadowing, caused by large vehicles, on outage probability of relaying scheme, and can thus be used to design a relay system for V2V communications with large vehicular obstructions. We note that the measurements were performed with two static devices, and one mobile device. This corresponds, e.g., to a situation in a traffic jam. A more general investigation would have both vehicles, and possibly the relay (if located on a bus) in motion. Such analysis requires a different measurement

setup and more extensive measurement campaigns, and will be subject for our future work.

## VI. ACKNOWLEDGMENTS

The work is supported by the National Natural Science Foundation of China under Grant 61501020, the China Postdoctoral Science Foundation under Grant 2016M591355, the Fundamental Research Funds for the Central Universities under Grant 2015RC025, and the State Key Laboratory of Rail Traffic Control and Safety under Grant RCS2016ZJ005.

## REFERENCES

- [1] A. F. Molisch, F. Tufvesson, J. Karedal, and C. F. Mecklenbrauker, "A survey on vehicle-to-vehicle propagation channels," *IEEE Wireless Communications*, vol. 16, no. 6, pp. 12–22, 2009.
- [2] R. He, O. Renaudin, V.-M. Kolmonen, K. Haneda, Z. Zhong, B. Ai, and C. Oestges, "A dynamic wideband directional channel model for vehicle-to-vehicle communications," *IEEE Transactions on Industrial Electronics*, vol. 62, no. 12, pp. 7870–7882, 2015.
- [3] A. F. Molisch, *Wireless communications 2nd ed.* Wiley, 2010.
- [4] Y. Ge, S. Wen, Y.-H. Ang, and Y.-C. Liang, "Optimal relay selection in IEEE 802.16 j multihop relay vehicular networks," *IEEE Transactions on Vehicular Technology*, vol. 59, no. 5, pp. 2198–2206, 2010.
- [5] M. J. Khabbaz, W. F. Fawaz, and C. M. Assi, "Probabilistic bundle relaying schemes in two-hop vehicular delay tolerant networks," *IEEE Communications Letters*, vol. 15, no. 3, pp. 281–283, 2011.
- [6] I. Dey, R. Nagraj, G. Messier, and S. Magierowski, "Performance analysis of relay-assisted mobile-to-mobile communication in double or cascaded Rayleigh fading," in *Proc. IEEE PacRim'11*, 2011, pp. 631–636.
- [7] M. F. Feteiha and M. Uysal, "Infrastructure-to-vehicle cooperative communications with decode-and-forward relaying," in *Proc. IEEE PIMRC'11*, 2011, pp. 804–808.
- [8] Z. Li, H. Hu, L. Jia, F. Li, and H. Wang, "Outage bound analysis in relay-assisted inter-vehicular communications," in *Proc. IEEE VTC'10*, 2010, pp. 1–5.
- [9] M. Seyfi, S. Muhaidat, J. Liang, and M. Uysal, "Relay selection in dual-hop vehicular networks," *IEEE Signal Processing Letters*, vol. 18, no. 2, pp. 134–137, 2011.
- [10] Z. Xu, L. Bernadó, M. Gan, M. Hofer, T. Abbas, V. Shivaldova, K. Mahler, D. Smely, and T. Zemen, "Relaying for IEEE 802.11 p at road intersection using a vehicular non-stationary channel model," in *Proc. IEEE WiVeC'14*, 2014, pp. 1–6.
- [11] T. Abbas, J. Kåredal, and F. Tufvesson, "Shadow fading model for vehicle-to-vehicle network simulators," in *Proc. 5th COST IC1004 Management Committee and Scientific Meeting*, 2012.
- [12] T. Abbas and F. Tufvesson, "Line-of-sight obstruction analysis for vehicle-to-vehicle network simulations in a two-lane highway scenario," *International Journal of Antennas and Propagation*, vol. 2013, 2013.
- [13] R. He, A. F. Molisch, F. Tufvesson, Z. Zhong, B. Ai, and T. Zhang, "Vehicle-to-vehicle propagation models with large vehicle obstructions," *IEEE Transactions on Intelligent Transportation Systems*, vol. 15, no. 5, pp. 2237–2248, 2014.
- [14] K. Amiri, Y. Sun, P. Murphy, C. Hunter, J. R. Cavallaro, and A. Sabharwal, "WARP, a unified wireless network testbed for education and research," in *Proc. IEEE MSE'07*, 2007, pp. 53–54.
- [15] R. He, A. F. Molisch, F. Tufvesson, Z. Zhong, B. Ai, and T. Zhang, "Vehicle-to-vehicle channel models with large vehicle obstructions," in *Proc. IEEE ICC'14*, 2014, pp. 5647–5652.
- [16] Y.-W. Hong, W.-J. Huang, F.-H. Chiu, and C.-C. J. Kuo, "Cooperative communications in resource-constrained wireless networks," vol. 24, no. 3. IEEE, 2007, pp. 47–57.
- [17] M. Torabi, W. Ajib, and D. Haccoun, "Performance analysis of amplify-and-forward cooperative networks with relay selection over Rayleigh fading channels," in *Proc. IEEE VTC'09*, 2009, pp. 1–5.
- [18] M. R. Souryal and B. R. Vojcic, "Performance of amplify-and-forward and decode-and-forward relaying in Rayleigh fading with Turbo codes," in *Proc. IEEE ICASSP'06*, 2006, pp. 681–684.
- [19] A. Paier, D. Faetani, and C. F. Mecklenbrauker, "Performance evaluation of IEEE 802.11 p physical layer infrastructure-to-vehicle real-world measurements," in *Proc. IEEE ISABEL'10*, 2010, pp. 1–5.